INTERNATIONAL JOURNAL OF MICROWAVE AND OPTICAL TECHNOLOGY,

VOL.2 , NO.2 , APRIL 2007

Absolute Characterization of EUV Radiation Generated By Discharge Produced Plasma (DPP) For Lithography Applications

H. Merabet[1,2*], R. Bista[2], R. Bruch[2], and S. Fülling[2]

[1] Mathematic and Sciences Unit, Dhofar University, Salalah 211, Sultanate of Oman
[2] Department of Physics, University of Nevada Reno, Reno, NV 89557 USA
Tel: +968-2322-5061, Ext. 486; Fax: +968-2322-5059/64; E-mail: merabet@du.edu.om

***Abstract*- The application of extreme ultraviolet (EUV) lithography in large-scale semiconductor chip manufacturing requires high power EUV radiation sources. The wavelength of the emission should be between 13 and 14 nm according to the 13.4 nm roadmap. To this end, a versatile microwave plasma-based EUV light source type Compact Electron Cyclotron Resonance Ion Source (CECRIS) has been recently built at Lawrence Berkeley National Laboratory (LBNL). In this paper, we present a detailed study of the generation of xenon (Xe) EUV light by the CECRIS using a 1.5 grazing incidence EUV monochromator that has been absolutely calibrated at the advanced Light Source (ALS). For diagnostic purposes, a theoretical study of Xe EUV line emission was performed based on relativistic Hartree-Fock approximation. A major outcome of this work is the absolute calibration of the EUV diagnostic system, which can be used for calibration of other industrial lithography sources.**

***Index Terms*- EUV Emission, Xenon Atomic Spectra, 13.4 nm, Plasma discharge, EUV Lithography.**

I. INTRODUCTION

Optical projection lithography is the technology currently being used to print the intricate patterns that define integrated circuits onto semiconductors wafers. Potential successors to optical projection lithography are being aggressively developed. These are known as “Next-Generation Lithographies” (NGL’s). Extreme Ultraviolet Lithography (EUVL) is one of the leading NGL technologies [1]. The source is an integral part of a EUVL tool. Such a source, as well as the EUVL tool, has to fulfill extremely high demands both technical and cost oriented.

The light production mechanism has been changed from conventional lamps and lasers to relatively high temperature emitting plasmas. While there are different methods to generate EUV radiation, such as synchrotrons, free electrons lasers, laser produced plasmas (LPP) and discharge produced plasmas (DPP), only the latter two prove to be economically viable solutions for EUVL [2].

For both LPP and DPP the EUV light is generated by hot (about 20-50 eV) plasma. In the case of LPP though, the emitting plasma is produced by focusing of the pulsed laser on the xenon target, while in the case of DPP the mechanism is a discharge pinching one. Depending on the choice of material of the target EUV generation might be broad-band, e.g. for Xe and Sn, or a line spectrum, e.g. Li. Gas discharge-produced plasma EUV sources are highly efficient because the electrical energy is directly converted to EUV light. However, they show limits with regard to the lifetime of the discharge electrode system and the achievable output power [2]. While substantial progress has been made in the field of EUV spectrometry, there is still a strong need for new concepts for stable, efficient gas discharge based sources such as CECRIS [3].

INTERNATIONAL JOURNAL OF MICROWAVE AND OPTICAL TECHNOLOGY,

IJMOT

VOL.2 , NO.2 , APRIL 2007

Currently, the most advanced lithographic tools used in high-volume manufacture employ deep-ultraviolet (DUV) radiation with a wavelength of 248 nm to print features that have line widths as small as 200 nm. But EUVL, which is under development, aims to utilize light of wavelength in the range of about 11-14 nm to shrink the size of printed features as small as 30 nm for integrated circuits manufacturing [4]. These EUV systems utilize a wavelength of about 13.4 nm (13.4 nm roadmap). Thus the reduced wavelength introduces several demanding challenges like (i) materials are strongly absorbent in the EUV region (ii) systems require high vacuum operation and (iii) EUV optical devices generally incorporate effective reflective surfaces based on multi-mirror technology [5]. Therefore EUVL requires technology advancement in the field of light source efficiency, mirror reflectivity, light source power, spectral purity, lifetime, and stability [6].

It is well recognized that magnetically assisted microwave produced plasmas have led to substantial improvements in the fabrication of electric components. Currently, ECRIS have been extensively applied to numerous low-pressure plasma processing applications such as etching, deposition and ion implantation [7]. Both experimental and theoretical investigations have suggested that ECRIS plasma environment are far from thermal equilibrium i.e. the electron distribution is strongly anisotropic [8]. Electron density, electron population temperature and ionic temperature are the relevant plasma parameters for such ECRIS. The measurement of highly charged ionic density is of great importance for understanding and upgrading such sources. These devices are very prominent candidates for the production of intense EUV radiation arising from the plasma confinement.

This work is divided into two sections. In the first part, we have described the calibration method of a 1.5 m grazing incidence monochromator with the light source of known frequencies at ALS of LBNL using beamline 6.3.2. Hence, we have established the calibration curve for monochromator for wavelengths ranging from 10 to 80 nm. In the second part we have used this calibrated monochromator for EUV diagnostics of a Compact ECRIS (CECRIS), also called a microwave plasma source. In particular, we have measured and identified numerous new EUV radiative lines structures arising from xenon ions at different ionization stages in the wide wavelength range of 10-80 nm. Since we have calibrated our monochromator, all of our observed data are normalized. Special attention was given to the wavelength of 13.4 nm region with lithographic applications.

II. EXPERIMENTAL APPARATUS

In the near future, EUVL is expected to replace existing lithography systems. It is anticipated that the generation of computer chip designs and fabrication of the semiconductor industry will switch to EUV lithography. Lithography, is basically a photographic process that allows more features to be integrated onto a computer chip. In this case, light is directed onto a mask-a sort of stencil of an integrated circuit pattern- and the image of that pattern is then projected onto a semiconductor wafer covered with light sensitive photoresist [9]. However, unlike visible lithography, EUVL and soft X-ray lithography uses much shorter wavelengths so that the chip components can be extremely small (down to a few nanometers, about 10 times the size of small molecules or large atoms). Thus, chips can be produced with significantly smaller feature size. Furthermore, as the wavelengths are relatively small, it becomes possible both to resolve smaller structures in EUV microscopy. In order to exploit these fascinating opportunities rapid advances in the development of efficient EUV light sources and EUV optical systems are very critical.

A. Electron Cyclotron Resonance Ion Source (ECRIS)

Particle accelerators—such as the cyclotron—use electromagnetic fields to accelerate different ions. To be accelerated, atoms and/or molecules need to become electrically charged (become ionized) by having some of their electrons

INTERNATIONAL JOURNAL OF MICROWAVE AND OPTICAL TECHNOLOGY,

VOL.2 , NO.2 , APRIL 2007

removed. Generally, the removal of electrons from neutral atoms is accomplished with ECRIS. In an ECR source, vapor or gases of the desired element is held in a specially designed magnetic field—a "magnetic bottle" long enough for the atoms to be ionized in collisions with electrons, which are kept in motion by microwaves. The magnetic bottle is shaped by circular coils at its top and bottom and a hexapole magnet (three "north poles" alternating with three "south poles") around the sides. The transmitters for the microwaves that heat the electrons run at several times the frequency of a household microwave oven.

A gas or vapor of the desired element enters at the top of the magnetic bottle. The corresponding ions gradually leak out at the bottom, from which point they are sent on to the cyclotron. A very tiny oven is available to heat metals and other solid elements to the gaseous stage. The ion sources are important because, in order to do an experiment in a reasonable amount of time, the accelerator should provide enough ions at the desired energy [10]. Schematic diagram of an ECRIS is given in Fig. 1.

The plasma in the ECRIS is confined in a magnetic trap formed by the electric currents flowing in the solenoids (axial confinement) and by the radial magnetic field produced by the hexapole magnet, which is made of permanent magnets or superconducting coils. The electrons in the plasma are resonantly accelerated when they pass the resonance zone where their girofrequency equals the frequency of the microwave injected into the plasma chamber. The originally neutral gas or metal vapor atoms are ionized in step-by-step collisions with fast electrons.

The use of ECRIS for production of intense beams of highly charged ions and EUV radiation has immensely grown over the last decade [11]. One main advantage of this kind of ion source is that in principle ions of all elements can be produced.

Furthermore, there are fewer parts in the ion

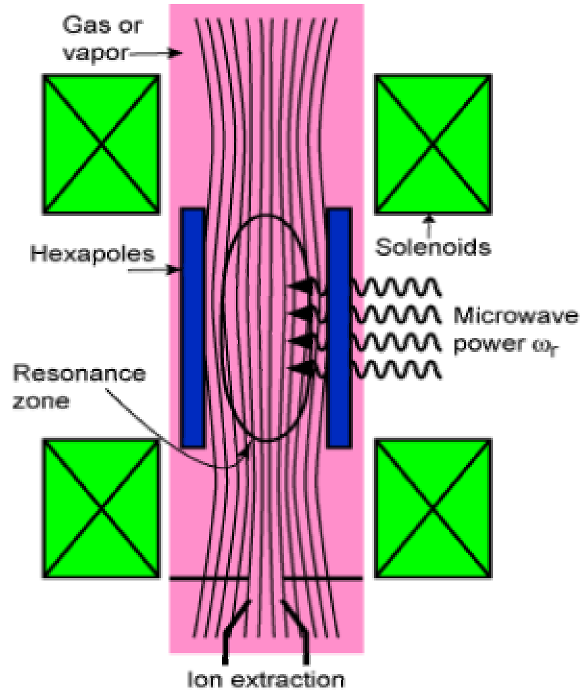

Fig. 1 Schematic diagram of an Electron Cyclotron Resonance ion source (ECRIS)

source, which can wear out with time like filaments. Therefore, stable ion beams can be realized for long periods (days - weeks) limited only by the material consumption of the used elements or gases. ECR ion sources work at a relatively low gas pressure and have a high ionization efficiency of the plasma, making them quite suitable for the production of ion beams and short wavelength radiations [12].

B. Basic Principle of Operation of ECRIS

ECRIS operates at low neutral gas pressure, typically 0.2-10 m torr. Low pressure reduces ion collisions in the substrate sheaths, which are necessary for anisotropic etching of the smaller and increasingly high aspect ratios features in modern integrated circuits. ECRIS also operate in the relatively high-density range of $n_i \approx 10^{11} - 10^{12} cm^{-3}$. Higher ion density implies higher ion-flux-driven processing rates which is important due to high ownership costs of lithography tools. Another beneficial property of ECRIS is low plasma potential, typically 15-30 eV without substrate biasing. However, there is

INTERNATIONAL JOURNAL OF MICROWAVE AND OPTICAL TECHNOLOGY,

VOL.2 , NO.2 , APRIL 2007

one main disadvantage. ECR tools require approximately several kilogauss of magnetic field, implying extra expense for power supplies, cooling power and floor space. A more detailed schematic of an ECRIS is shown in Fig. 2 [13].

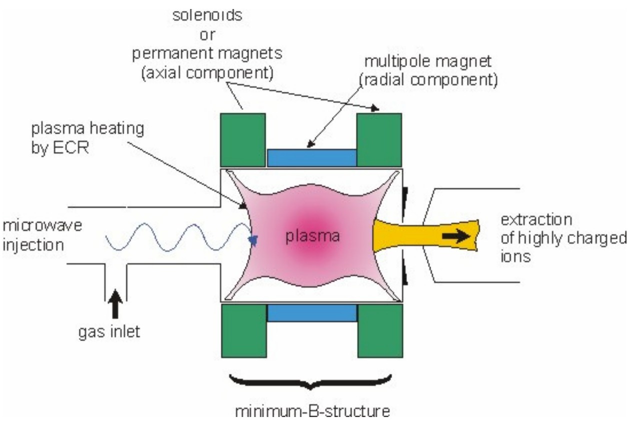

Fig. 2. Schematic view of Ultra Compact Microwave Plasma Source (Light Source)

A steady state magnetic field is generated by the permanent magnets surrounding the plasma. The magnetic field is typically of the order of a few kilogauss or more. When electrons move in a magnetic field they gyrate around the magnetic field lines due to the Lorentz force. The gyration frequency is called the cyclotron frequency ω_{cyc}. Microwaves are introduced into the source chamber through a dielectric vacuum window by a coupling structure. Quartz is the most common window material but alumina is also used in some cases. The most common microwave frequency used is in the range 2.45- 28 GHz. The rectangular waveguide used is typically of the dimensions 3.8 cm x 7.6 cm. If microwave radiation of the same frequency propagates into such a region, the electrons are resonantly accelerated or decelerated depending on the phase of their transversal velocity component with respect to the electric field vector. Most ECRIS operate at power levels in the range of 0.1 and 1.5 kW although 5 kW systems are now commercially available at 2.45 GHz [14].

C. Calibration of the 1.5 m gazing incidence monochromator

The major accomplishment of this work is the successful calibration of our 1.5 m grazing incidence monochromator. For this purpose we have used the beamline 6.3.2 of ALS which is primarily designed for the purposes of calibration, optics testing and spectroscopy. The schematic of beamline 6.3.2 is shown in Fig 3. [15]. High spectral resolution is obtained using a variable- line spaced (VLS) plane grating

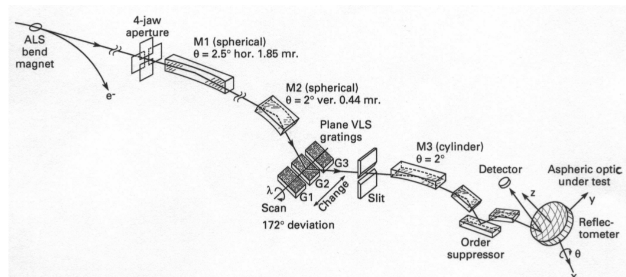

Fig. 3. A schematic of beamline 6.3.2 at ALS

monochromator. The monochromator, designed and constructed by the Center for X-ray Optics, has a very compact design with three variable-line-spaced gratings, no entrance slit, and a fixed exit slit. Entrance-slitless operation is possible because of the small size and high stability of the ALS beam. A vertically deflecting spherical mirror converges the EUV beam onto the monochromator grating. Aberrations of the mirror are corrected by the varied line spacing of the grating, so that the spectral resolving power of 7000 is determined primarily by the small size of the ALS beam. The wavelength is scanned by simple rotation of the grating with respect to the fixed monochromator exit slit. The light is focused onto the sample by the first horizontally deflecting mirror and a bendable focusing mirror downstream from the monochromator. High spectral purity is achieved using a combination of filters and a triple mirror “order-suppressor”. The space downstream from the reflectometer is used as additional experimental stations for a variety of applications, including spectroscopic studies in atomic, molecular, and material science [15].

During our experimental set up, the main difficulties that we faced was the alignment of our monochromator with the end station of

INTERNATIONAL JOURNAL OF MICROWAVE AND OPTICAL TECHNOLOGY,

IJMOT

VOL.2 , NO.2 , APRIL 2007

beamline 6.3.2. Perfect alignment is essential for correct reading. We have aligned our monochromator with the station after reflectometer. The monochromator connected at the end station is pictured in Fig 4.

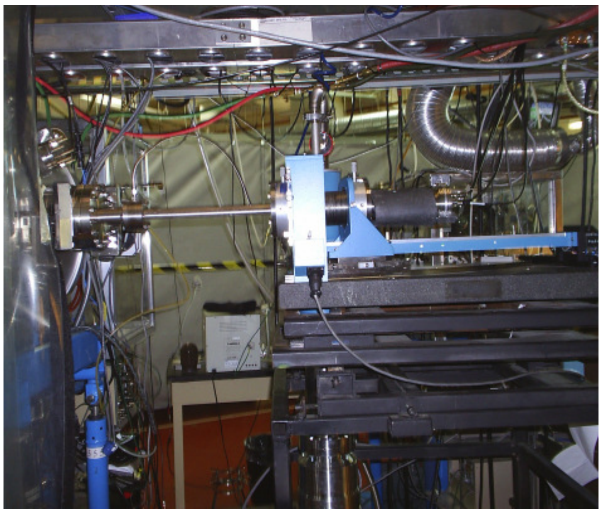

Fig. 4. 1.5 m grazing incidence monochromator connected with end station at ALS beamline 6.3.2

We recorded several measurements in the 13-30 nm wavelength range with highly monochromatic synchrotron light in order to study the wavelength dependence efficiency of our EUV monochromator. The calibration procedure has been described in detail by Bista and coworkers [16]. Hence, only a brief description of calibration procedure is summarized below. The flux (ϕ_0) of incident photons was measured with a photodiode before the entrance of our EUV monochromator so that absolute value was obtained before and after each set of measurements. Particularly, we measured the incident photon flux for four known specific wavelengths of 13.4, 18.4, 25.4 and 30.4 nm, respectively. Photons emitted by the synchrotron light source are directed to the entrance slit of the monochromator with slit widths varying between 5 μm to 3 mm, depending on the desired resolution to be achieved. Then they were dispersed by a reflection grating at an angle of incidence of 88^o. The 1.5 meter radius concave reflection grating with 600 grooves/mm and a blaze angle of 5^o was positioned on a Rowland circle mounting allowing measurements within the investigated wavelength range. To find the corresponding final photon flux, measured data points were fitted by a Gaussian line profile and subsequently analyzed by using Origin 7.0 program. The central peak and the full width at half maximum (FWHM) allowed us to determine the corresponding measured final flux (ϕ_f) traversing the EUV monochromator. For each measured wavelength, we have divided the final flux (ϕ_f) by the incident flux (ϕ_0). This ratio corresponds to the efficiency of our EUV detection system for a particular wavelength. We made several independent measurements for each wavelength by changing measurements parameters as a function of integration time, charge normalization, number of steps etc. Furthermore averages of resulting efficiencies were obtained and the specific absolute count rate n (number of photons/sec) was determined by dividing the measured flux by the corresponding efficiency (η) for a particular wavelength ($n = \phi_f / \eta$). The flux ϕ_0 of incident photons was measured with a photodiode before the entrance of the monochromator so that absolute values were obtained before and after each set of measurements. The corresponding parameters of the calibration are listed in the table 1. The EUV monochromator was controlled by a versatile CAMAC-PC system for data acquisition and control [8]. A complete description of this experimental setup is given by Bruch and co-workers [20-26].

The sensitivity of our 1.5 m grazing incidence monochromator system for 23 nm to 58 nm wavelength range has been established earlier by Fülling and co-workers [17]. In their work, they had calibrated the 1.5 m monochromator with respect to the 2.2 m grazing incidence monochromator in Bochum (Germany) that was equipped with a gold coated concave grating (600 grooves/mm) and a channeltron detector. The overall accuracy of this calibration was estimated to be within 10% to 15% [25].

INTERNATIONAL JOURNAL OF MICROWAVE AND OPTICAL TECHNOLOGY,

VOL.2 , NO.2 , APRIL 2007

Table 1: Determination of the absolute flux (number of photons/sec) for different wavelengths investigated at the ALS light source

λ (nm)	Incident Photon Current (A)	Conversion factor (A/W)	Diode Power (W)	Flux number (photon/s)
13.4	0.776	0.145858	5.320	3.590E+17
18.4	0.586	0.148881	3.936	3.648E+17
25.4	0.059	0.143462	0.411	5.266E+16
30.4	0.023	0.1462035	0.155	2.387E+16

Using the previously determined sensitivity, the dependence of the efficiency from 13 to 58 nm was obtained. Moreover, a spline extrapolation has enabled us to extend the covered range to lower as well as higher wavelengths so that a curve for the 10 nm to 80 nm regions was achieved. Finally we have obtained calibration curve (sensitivity) for our monochromator for wide wavelength range of 10-80 nm (Fig. 5).

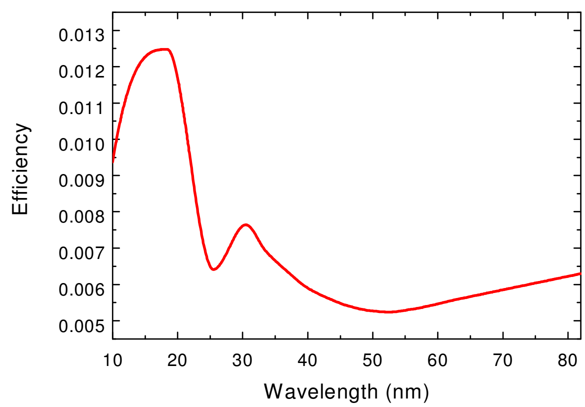

Fig. 5. Calibration curve for 1.5 m monochromator for wavelength range of 10-80 nm range

D. EUV emission from Plasma Sources

The prototype ECRIS used for our experiments was developed by the Plasma and Ion Source Technology Group under the guidance of Dr. Kao-Leung at LBNL [5]. This simple ECRIS is cost effective, compact, and efficient. It has been designed to produce intense EUV radiation useful for lithography applications. It uses the same method of microwave heating as conventional ECR sources but employs a simpler permanent magnet ring structure to produce a dipole field instead of a more complex electromagnet and permanent magnet structure [18]. To obtain reasonable intensities of Xe^{q+} ions, C-band (5.9 – 6.4 GHz) microwaves were used. The ECR plasma heating at 6.4 GHz requires ~ 2200 Gauss magnetic field in the source in order to couple the microwaves efficiently to the plasma. The magnetic field is produced using permanent magnets. By carefully designing the permanent magnet geometry, a uniform volume resonant magnetic field can be obtained. A movable magnet yoke provides a way to fine tune the B-field.

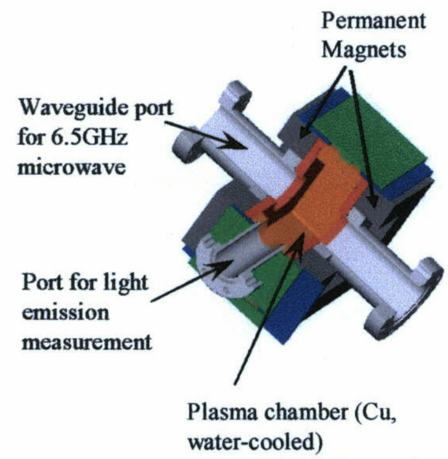

Fig. 6. 3-D Schematic of the CECRIS with its components

In this study the EUV emission of the CECRIS has been measured by a 1.5 m Grazing Incidence Monochromator under the condition of medium and high wavelength resolution. To discriminate between the highly excited Xe spectral components associated with different charge states, the EUV spectrometer is connected to the plasma source chamber via a glass capillary system in order to maintain high vacuum at the monochromator system, while the source reaches a gas pressure of about 1 mTorr (see Fig. 7). In addition, this configuration has allowed applying high voltage to the EUV source independently from the monochromator. The photons emitted in the source chamber enter a 500 mm long, 4 mm inner diameter glass capillary before passing through the entrance slit. With both entrance and exit slits set at 100 μm, a resolution of 0.1 nm at

INTERNATIONAL JOURNAL OF MICROWAVE AND OPTICAL TECHNOLOGY,

VOL.2 , NO.2 , APRIL 2007

wavelength of about 30 nm is obtained, corresponding to a spectral resolution of $(\lambda/\Delta\lambda) \approx 304$.

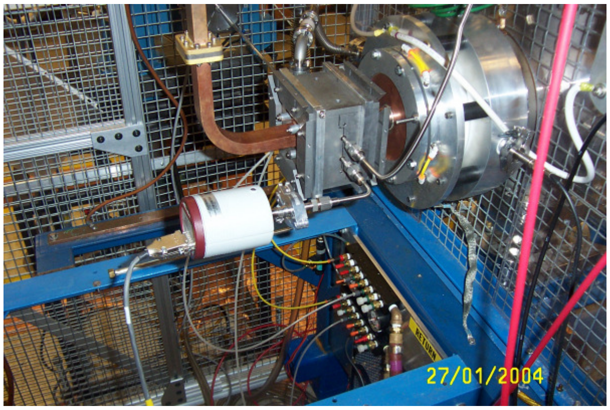

Fig. 7. Compact Microwave Plasma Generator (CECRIS) in the test bend

III. RESULTS AND DISCUSSION

In the second part of this work, we present our investigations on the CECRIS. Spectroscopic measurements were performed of the plasma using xenon gas. The experiments were carried out under low, medium and high-resolution experimental conditions. In addition, the emission spectra of Xe ions (from Xe^{+} to Xe^{10+}) have been calculated for the wavelength interval λ = 10-80 nm. The calculations have been carried out within the relativistic Hartree-Fock (HF) approximation [18]. From 25 to 38 configurations, including the ground state and single excited states, were taken into account in the configuration interaction calculations for each ion. Configurations were generated by excitation of one of 5p, 5s, 4d, 4p, 4s electrons to shells with n = 5, 6, 7. Electron orbital with l = s, p d, f and g were considered. Configurations with two excited electrons were not included in the calculations at this stage. For Xe^{1+} to Xe^{5+} ions, configurations with 4d shell ($4d^9$) are important, for Xe^{6+} and Xe^{7+} ions configurations with 4d and 5snl or nl play a major role. For Xe^{8+} - Xe^{10+} ions, configurations with unfilled 4d shell have to be considered for the interpretation of the experimental data. Number of possible dipole transitions in the region 10-100 nm is very high (thousands of lines for each xenon ion).

The interval 10-22 nm has less spectral line compared to the 40 – 80 nm regions. However, even in this case we have to consider hundreds of lines for each ion disregarding weak transitions with small gf values (oscillator strength times statistical weight) [18]. The detailed results of these calculations are presented elsewhere [19-26]. We have measured various spectral lines between the wavelength ranges of 10-80 nm. Then, we have normalized each of our data by dividing experimental data with the respective efficiency of our monochromator giving the total flux of the system.

The peak fitting analysis was performed using the software Origin (version 7.0). The measured spectra were fitted by means of a standard Gaussian peak shape. A linear function was used to remove the residual background. With the measured high signal-to noise ratio, even weaker lines could be resolved with higher accuracy. Firstly, the second derivative spectrum was generated which was used to identify the hidden peaks. Secondly, the peaks obtained from the second derivative spectrum, by finding all local minima, were fitted allowing centroids, widths and peak amplitudes to vary simultaneously in the process generating the best spectral fit to the data.

Fig. 8 illustrates a high resolution Xe spectrum in the wavelength range 10-16 nm range, where we have found total of major 32 spectral peaks corresponding to different transitions. For clarity, only few prominent lines are shown.

The dominating xenon lines are attributed to Xe^{8+}, Xe^{9+}, and Xe^{10+} initial charge states. In addition we have assigned some O^{3+}, O^{4+}, O^{5+} transitions due to residual oxygen gas. We have also found contributions from N^{4+}, N^{5+} transitions due to the virtual leaks of the source. The dominant Xe lines arising from the excitation of Xe^{8+} ions stem from configurations ($4d^9nl$) with n = 4, 5 and 6 decaying to the lower ($4d^{10}$) ^1S state. The major contributions from Xe^{9+} photon decays

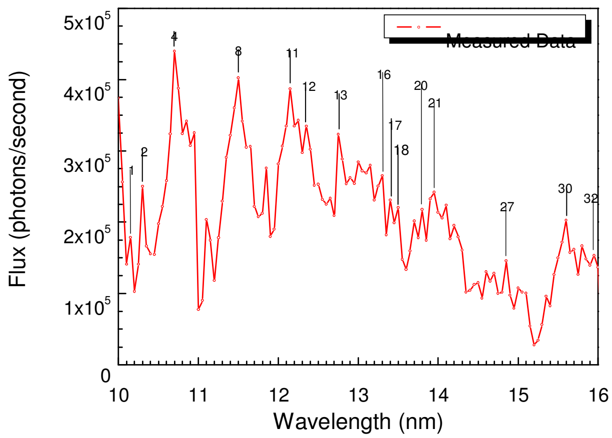

Fig. 8. High resolution xenon EUV spectrum between 10-16 nm. Continuous background was subtracted.

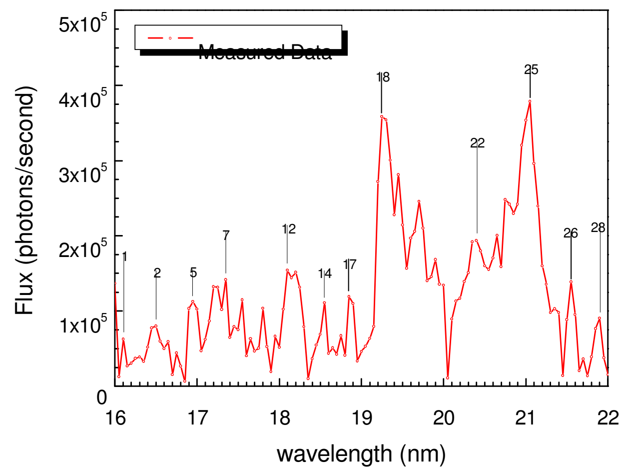

Fig. 9. High resolution xenon EUV spectrum between 16-22 nm. Continuous background was subtracted.

should result from ($4d^8nl$) excited states with n = 4 and 5 decaying to the $(4d^9)^2D$ lower state. Another important finding is the excitation of Xe^{10+} ions due to ($4d^7nl$) configurations with n = 4 and 5 decaying to different lower states arising from ($4d^8$) core. We further note that the most pronounced peak structure centered at 10.70 nm may be attributed to $(4d^8)^3F$-($4d^95p$) radiative decay. One more strong line occurs at 11.50 nm and could be assigned to $(4d^9)^2D$-($4d^84f$) fine structured transitions. An additional significant line occurs at 12.15 nm and has been tentatively assigned to $(4d^{10})^1S$-$(4d^96p)^1P$ and J equals 0 and 1 fine structured transition. The 13.4 nm peak is dominated by Xe^{10+} ionic states [27]. The theoretical Hartree-Fock calculations for different wavelengths are in close agreement with the obtained experimental results.

A further prominent high resolution section of the Xe spectrum in the wavelength range of 16-22 nm is displayed in Fig. 9. A resolution of about 270 was obtained for this spectrum using the 600 grooves/mm grating. In this case, we have absolutely normalized each of our data by dividing it with the respective efficiency of our monochromator to calculate the total flux of the system. In this range, we have designated the most prominent spectral lines from 1 to 28. The theoretical Hartree-Fock calculations for this wavelength range are also in close agreement, with our experimental findings. Only some of the prominent peaks are shown in Fig. 9 for clarity.

Furthermore, we have investigated the xenon spectrum in the higher wavelength region to gain more information about the different excitation and de-excitation processes. In Fig. 10, we have plotted a medium resolution xenon spectrum between 40-60 nm. The dominant spectral features observed are denoted 1 to 39. It has been observed that the spectrum is dominated by Xe^{q+} (q=1-10) ions, however, residual contribution from oxygen and nitrogen ions are also present.

A detailed comparison of the observed line intensities and peak positions with previously predicted values is given elsewhere [23]. The most dominant Xe line structures arise from a variety of ions such as Xe^{2+}, Xe^{5+} Xe^{6+}, Xe^{8+} and Xe^{9+}. Additional observed line structures could be assigned to N^{4+}, O^{2+}, O^{3+} and O^{5+} fine structure transitions. Interesting features observed in this spectrum are radiative decays among ($4d^9nl$) and ($4d^9nl$`) transitions for n = 5. The most pronounced peak structure centered at 53.80 nm may be attributed to $(5s5p^2)^2D$-(5s5p5d) decay. Finally, Fig. 11 indicates the high resolution Xe spectra for the segment between 60 and 80 nm. More intense peaks are assigned from 1 to 43 but only few are shown. This spectrum was measured using the 600 grooves/mm grating producing a resolution of 170 and the continuous background was subtracted. This portion of the spectrum can be predominantly assigned to radiative transitions arising from Xe^{2+}, Xe^{3+}, Xe^{5+} and Xe^{6+} excited states. Most distinct peak structures are centered at 72.15 and 72.32 nm and may be attributed to $(5s5p)^3P$-$(5p^2)^3P$ and $(5s5p)^3P^2$-$(5p^2)^3P$, respectively. Moreover several peaks due to O^{2+}, O^{4+}, O^{7+}, N^{4+}, N^{6+} and N^{3+} have been identified as well [23].

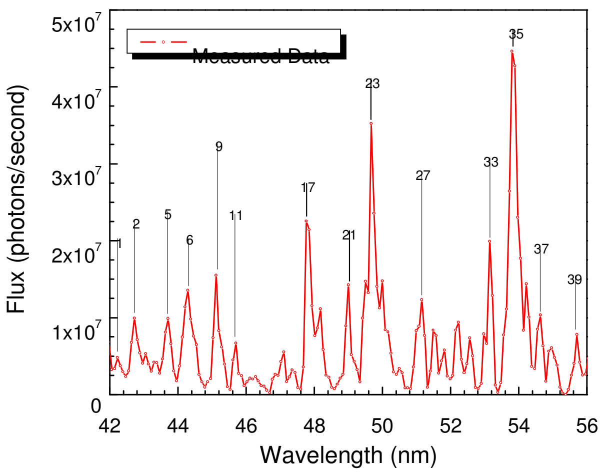

Fig. 10. High resolution Xe EUV spectrum between 40-60 nm. Continuous background was subtracted.

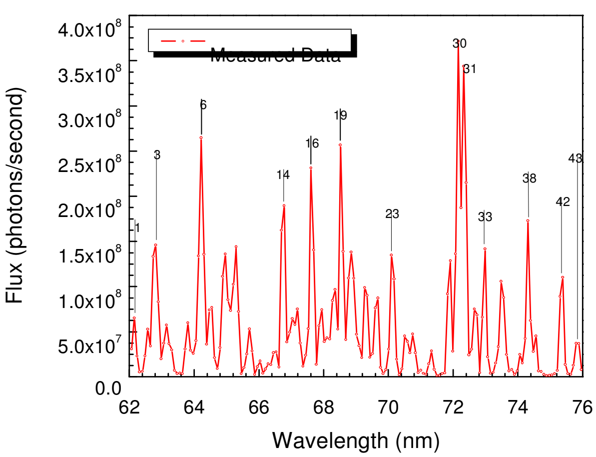

Fig. 11: High resolution Xe EUV spectrum between 60-80 nm. Continuous background was subtracted.

VI. CONCLUSION

In summary, the experiments discussed in this paper are associated with the calibration of a 1.5 m grazing incidence monochromator and the study of EUV emission from a compact microwave plasma source using this monochromator. The absolute calibration of the EUV measurement system using light source of known frequencies at ALS is a major accomplishment of this endeavor. Especially, we were able to depict an extended calibration curve for our EUV monochromator for a wide wavelength range of 10-80 nm. Furthermore, we have studied the generation of EUV radiation by a novel Compact Electron Cyclotron Resonance Ion Source (CECRIS). Several spectra were recorded using 600 grooves/mm grating with different resolution conditions. We have also identified many fine structure transitions utilizing our theoretical database.

Particular attention was devoted to the 13.4 nm roadmap region that has significant EUV lithography applications. We have shown in this study that the cost-effective, stable, and extremely compact light source can produce highly charged Xe EUV radiation in the vicinity of the 13 nm region. Especially, we have provided evidence that Xe^{10+} ions could be produced by such a simple source. However we have found that the intensity and brightness of this source should be increased to fit to the high power requirements of lithography applications. Finally, now we have absolutely calibrated EUV detection system which can be utilized in future for further investigation and diagnostics of plasma light sources. Moreover, the intensity of such type of ECRIS might be further improved by using advanced EUV optical systems such as polycapillary lenses [28], which make them more suitable for EUVL.

ACKNOWLEDGMENT

This project has been supported, in part, by Applied Photonics Worldwide (APW) Inc., Reno Nevada. The authors wish to thank Dr. K.L.

INTERNATIONAL JOURNAL OF MICROWAVE AND OPTICAL TECHNOLOGY,

VOL.2 , NO.2 , APRIL 2007

Leung and Dr. E. Gullikson and their research team members from Ion Beam Technology Group and ALS, LBNL respectively for their continuous support to accomplish this endeavor.

REFERENCES

[1] M. Putero-Vuaroqueaux and B. Vidal, "Extreme-ultraviolet multilayer mirrors deposited using radio-frequency-magnetron sputtering: the influence of self-bias voltage on reflectivity and roughness", J. Phys.: Condens. Matter 13, pp. 3969-3976, 2001.

[2] Uwe Stamm, "Extreme ultraviolet light sources for use in semiconductor lithography-state of the art and future development", J. Phys. D: Appl. Phys. 37, pp.3244-3253, 2004.

[3] R. Lebert, "Preliminary results from key experiments on sources for EUV lithography", Microelectronic Engineering, pp. 57-58, 2001.

[4] J.E. Bjorkholm, "EUVL – The Successor to Optical Lithography", Advanced Lithography Department, Intel Corporation, 2002.

[5] K.-L. Leung., V. Bakshi., R. Bruch, S. Hahto , Ji Q., S. Kondagari, H. Merabet., J. Reijonen and T. Schenkel, "The generation of EUV light with a compact ECR source", Ion Beam Technology Group, Berkeley Lab, 2004.

[6] "Light for the next chip generators", Fraunhofer magazine, pp. 2, 2002.

[7] www.phys.uit.no/~ane/Menga/properties.html.

[8] M .N. Rosenbluth and S R. Zagdeev, "Handbook of Plasma Physics", North-Holland, 1991.

[9] http://www.llnl.gov/str/Sween.html.

[10] http://www.nscl.msu.edu/tech/ionsource.html.

[11] D. Attwood, "Soft X-rays and Extreme Ultraviolet Radiation", Cambridge University Press, 2002.

[12] R. Geller, "Electron Cyclotron Resonance Ion Sources and ECR Plasmas", IOP Publishing Ltd, Bristol, 1996.

[13] D. Hitz *et al.*, "Fundamental aspects of ECRIS from classical to large superconducting devices", AIP, 2000.

[14] http://www.lbl.gov/Tech-Transfer.

[15] http://www-cxro.lbl.gov/als6.3.2.

[16] R. Bista, "Absolute calibration of a 1.5 m Grazing Incidence Monochromator for Extreme Ultraviolet (EUV) diagnostics of a plasma source", MS Thesis, Dept. of Physics, University of Nevada, Reno, USA, December 2005.

[17] S. Fuelling, "Excitation and ionization-excitation of helium in fast ion-atom collisions", PhD. thesis, Dept. of Physics, University of Nevada, Reno, USA, May 1991.

[18] R. D. Cowan "The theory of atomic structure and spectra", University of California Press, Berkeley, 1981.

[19] H. Merabet, S. Kondagari, R. Bruch, S. Fülling, S. Hahto, K-L. Leung, J. Reijonen, "EUV emission from xenon in the 10-80 nm wavelength range using a compact ECR ion source", 18th International Conference on the Application of Accelerators in Research & Industry, Denton, USA, October 10-15, 2004 (invited talk).

[20] S. Kondagari, H. Merabet, R. Bruch, S. Fülling, S. Hahto, K-L. Leung, J. Reijonen, "EUV spectroscopy of hollow ionic states using an Electron Cyclotron Resonance Ion (ECRIS)", 18th International Conference on the Application of Accelerators in Research & Industry, Denton USA, October 10-15, 2004 (Poster).

[21] H. Merabet, S. Kondagari, R. Bruch, S. Fülling, S. Hahto, K-L. Leung, J. Reijonen, "EUV emission from xenon in the 10-80 nm wavelength range using a compact ECR ion source", Nucl. Instr. Meth. B 241, pp. 23-29, 2005.

[22] H. Merabet, R. Bista, C. Schubert, S. Fülling, R. Bruch, A.L. Godunov, "Characterization of Extreme Ultraviolet (EUV) emission from xenon generated using a compact plasma-discharge source for lithography applications", SPIE Proceeding, Vol. 5918, pp. 102-113, 2005.

[23] H. Merabet et al., "Spectroscopic studies of xenon EUV emission in the 40-80 nm wavelength range using an absolutely calibrated monochromator", unpublished, 2006.

[24] H. Merabet, M. Bailey, R. Bruch, J. Hanni, S. Bliman, D. V. Fursa, I. Bray, K. Bartschat, H. C. Tseng, and C. D. Lin., "Cross sections and collision dynamics of the excitation of (1snp) $^1P^o$ levels of Helium, n = 2-5, by intermediate and high velocity electron, proton, and molecular ion (H_2^+ and H_3^+) impact", Phys. Rev. A 64, pp. 012712, 2001.

[25] M. Bailey, "A polarization study of the Extreme Ultraviolet Emission from Helium following electron impact utilizing a multilayer mirror polarimeter", PhD. Thesis, Dept. of Physics, University of Nevada, Reno, USA, May 1997.

[26] M. Bailey, R. Bruch, E. Rauscher and S. Bliman, "Cross sections for the ionization-excitation of helium by fast electrons and H^+, H_2^+ and H_3^+ ions: (np) $^2P^0$ levels, n=2-5", J. Phys. B 28, pp. 2655, 1995.

[27] S. S. Churilov, Y. N. Joshi, "Analysis of the $4p^64d^84f$ and $4p^54d^{10}$ configurations of Xe X and some highly excited levels of Xe VIII and Xe IX ions", Physica Scripta 65, pp.40, 2002.

[28] M. Bargheer *et al*.," Comparision of focusing optics for femtosecond X-ray diffraction", Appl. Phys B 00, pp. 1, 2005.